Journal Pre-proofs

Native and foreign mitochondrial and nuclear encoded proteins conform the OXPHOS complexes of a holoparasitic plant

Leonardo M. Gatica-Soria, Luis F. Ceriotti, Laura E. Garcia, M. Virginia Sanchez-Puerta

PII: S0378-1119(21)00771-X
DOI: https://doi.org/10.1016/j.gene.2021.146176
Reference: GENE 146176

To appear in: *Gene Gene*

Received Date: 13 August 2021
Revised Date: 2 November 2021
Accepted Date: 6 December 2021

Please cite this article as: L.M. Gatica-Soria, L.F. Ceriotti, L.E. Garcia, M. Virginia Sanchez-Puerta, Native and foreign mitochondrial and nuclear encoded proteins conform the OXPHOS complexes of a holoparasitic plant, *Gene Gene* (2021), doi: https://doi.org/10.1016/j.gene.2021.146176

Native and foreign mitochondrial and nuclear encoded proteins conform the OXPHOS complexes of a holoparasitic plant

Leonardo M. Gatica-Soria[1,2], Luis F. Ceriotti[1,2], Laura E. Garcia[1,2] & M. Virginia Sanchez-Puerta*[1,2]

[1]IBAM, Universidad Nacional de Cuyo, CONICET, Facultad de Ciencias Agrarias, Almirante Brown 500, Chacras de Coria, M5528AHB, Mendoza, Argentina.
[2]Facultad de Ciencias Exactas y Naturales, Padre Jorge Contreras 1300, Universidad Nacional de Cuyo, M5502JMA, Mendoza, Argentina.

*Author for correspondence:
M. Virginia Sanchez-Puerta
Email: mvsanchezpuerta@fca.uncu.edu.ar
IBAM, Universidad Nacional de Cuyo, CONICET, Facultad de Ciencias Agrarias, Almirante Brown 500, Chacras de Coria, M5528AHB, Mendoza, Argentina.
Phone +54 9 (261) 4135000 ext. 1307.

ABSTRACT

The intimate contact between the holoparasitic plant *Lophophytum mirabile* (Balanophoraceae) and its host plant (Fabaceae) facilitates the exchange of genetic information, increasing the frequency of horizontal gene transfer (HGT). *Lophophytum* stands out as it acquired a large number of mitochondrial genes (>20) from its legume host that replaced the majority of the native homologs. These foreign genes code for proteins that form multisubunit enzyme complexes, such as those in the oxidative phosphorylation system (OXPHOS) and cytochrome c maturation (ccm) system, together with dozens of nuclear-encoded subunits. However, the existence and the origin of the nuclear subunits that form the major part of the OXPHOS and ccm system in *Lophophytum* remain unknown. It was proposed that nuclear-encoding genes whose products interact with foreign mitochondrial proteins are also foreign, minimizing the incompatibilities that could arise in the assembly and functioning of these multiprotein complexes. We identified a nearly complete set of OXPHOS and ccm system subunits evolving under selective constraints in the transcriptome of *Lophophytum,* indicating that OXPHOS is functional and resembles that of free-living angiosperms. Maximum Likelihood phylogenetic analyses revealed a single case of HGT in the nuclear genes, which results in mosaic OXPHOS and ccm system in *Lophophytum*. These observations raise new questions about the evolution and physiology of this parasitic plant. A putative case of cooperation between two foreign (one mitochondrial and one nuclear) genes is presented.

Keywords*:* BALANOPHORACEAE*,* HORIZONTAL GENE TRANSFER, LOPHOPHYTUM, MTDNA, OXIDATIVE PHOSPHORYLATION

1. INTRODUCTION

Parasitic plants originated 12 times independently from free-living angiosperms (Nickrent, 2020). One of these lineages is the sandalwood order (Santalales), a monophyletic group that presents a wide variety of lifestyles, including autotrophic, hemiparasitic, and holoparasitic plants. Within the Santalales, holoparasitism arose in two lineages independently: Balanophoraceae *sensu stricto* and Mystropetalaceae (Su et al., 2015). The family Balanophoraceae *sensu stricto* encompasses 14 genera of obligate root holoparasites predominantly distributed in tropical regions (Nickrent, 2020; Su et al., 2015). Extraordinary properties associated with the molecular evolution of the organelles in members of this family have been recently reported. Plastid genomes in the Balanophoraceae exhibit high substitution rates, extreme AT content and two genetic code changes (Ceriotti et al., 2021; Schelkunov et al., 2019; Su et al., 2019). The mitochondrial genome is only known for *Lophophytum* and *Ombrophytum*, both of which show evidence of large-scale horizontal gene transfer (HGT) events mainly from their host plants (Roulet et al., 2020; Sanchez-Puerta et al., 2019, 2017).

Lophophytum mirabile subsp. *bolivianum* (Balanophoraceae) lives in northwestern Argentina, Bolivia and Paraguay, parasitizing roots of mimosoid legumes of the family Fabaceae (Hansen, 1980) (Sato, 2014). The intimate contact between the holoparasite and its host facilitates the movement of genetic information, increasing the frequency of HGT (Sanchez-Puerta et al., 2017). *Lophophytum* stands out among the frequent horizontal transfers involving plant mitochondria because of the replacement of 60% of its mitochondrial genes by host-derived homologs (Roulet et al., 2020; Sanchez-Puerta et al., 2019, 2017). Moreover, foreign genes are considered functional in the recipient mitochondria based on three lines of evidence, including significant transcription levels, accurate intron splicing, and efficient RNA editing of foreign homologs (Garcia et al., 2021). Among the functional foreign genes, there are several involved in the oxidative phosphorylation system (OXPHOS) and in the cytochrome c maturation (ccm) system, which are composed of multisubunit complexes formed by proteins encoded in the nuclear and mitochondrial genomes (Gualberto and Newton, 2017). Therefore, the OXPHOS and ccm system in *Lophophytum* contain foreign and native mitochondrial-encoded subunits (Sanchez-Puerta et al., 2017), while the presence and the origin of the dozens of nuclear-encoded subunits that form the major part of these systems remain unknown, with one exception -SDH3- (Garcia et al., 2021).The presence of foreign functional mitochondrial genes that interact with nuclear components could generate cytonuclear incompatibilities resulting in an aberrant or deficient OXPHOS system in *Lophophytum*. A reduced respiratory capacity has been reported for other parasitic eukaryotes (Santos et al., 2018). Among angiosperms, hemiparasites of the genus *Viscum* (Santalales) show reduced ATP production due to the absence of OXPHOS complex I and the use of alternative oxidases (Maclean et al., 2018; Senkler et al., 2017). *Lophophytum* has not been subjected to physiological studies and the nuclear genes encoding OXPHOS subunits have not been analyzed to date. A deficient OXPHOS system may imply that a few or many of the nuclear-encoded proteins involved in mitochondrial respiration are missing or evolving under genetic drift. Alternatively, it is possible that those subunits encoded in the nuclear genome that interact with mitochondrial proteins of foreign origin are also foreign, minimizing the incompatibilities that could arise in the assembly and functioning of these multiprotein complexes. Conversely, those nuclear-encoded proteins that interact with native mitochondrial-encoded proteins would be native.

Given that a major fraction of the mitochondrial subunits of protein complexes are foreign in *Lophophytum*, this species is an interesting model to study the evolution and impact of HGT on nuclear-encoded subunits that form part of mitochondrial complexes. In this study, we aim to i) assess the

completeness of OXPHOS complexes in *Lophophytum*; ii) evaluate the impact of HGT on these nuclear-encoded genes; iii) examine whether these nuclear genes are subjected to natural selection as indirect evidence of functionality; and iv) discuss the implications on the physiology and evolution of this parasitic plant.

2. MATERIALS AND METHODS

2.1. Transcriptomic data

The RNA sequence data of *Lophophytum mirabile* was obtained from NCBI (Bioproject PRJNA601125; Garcia et al., 2021). Briefly, total RNA extraction was performed from male and female flowers of an individual of *Lophophytum* collected from the Parque Nacional Calilegua (Jujuy, Argentina). Total RNA was treated with Ribo-Zero to remove ribosomal RNA. RNA sequencing (RNAseq) was performed with Illumina Hiseq2500 technology at Macrogen (Korea) and a total of 562,330,328 paired sequences of 101 bp in length with an insert size of 138 bp were obtained. The downloaded RNAseq data set was curated with Trimmomatic (Bolger et al., 2014) and assembled using Trinity v.2.8.4 (Grabherr et al., 2011). A BUSCO analysis of nearly universal single copy orthologs in eukaryotes, embryophytes, and eudicots indicated that the transcriptome was quite complete considering the holoparasitic nature of *Lophophytum* (Garcia et al., 2021).

We performed BLASTn and tBLASTn searches available at NCBI using CDS sequences of *Arabidopsis* nuclear genes (Table S1) as bait to obtain homologous genes in the *Lophophytum* transcriptome. Based on exploratory searches, we selected those transcripts with hits showing an identity greater than 40% and query coverage above 60% to make sure that we did not miss any homolog. We identified ORFs using the GETORF program (EMBOSS: GETORF) and verified if they correspond to homologs of the *Arabidopsis* gene used as query by making reciprocal BLASTn searches (Data set 1). Query sequences were obtained using the *Arabidopsis* gene identifier for the subunits of the OXPHOS complexes, cytochrome c, alternative oxidoreductases, and the maturation system of type c cytochromes listed by (Meyer et al., 2019), not considering the proposed subunits whose associations to the complexes have not been confirmed.

2.2. Phylogenetic analyses

To infer the phylogenetic relationships of *Lophophytum* nuclear genes, multiple sequence alignments were generated. Nuclear nucleotide sequences from 25 diverse angiosperms were obtained from GenBank databases by performing BLASTn searches against 'refseq_representative_genomes' (Table S1), using *Arabidopsis* nucleotide sequences as query. Again, those BLAST hits with an identity percentage greater than 40% and a coverage percentage above 60% were selected and the complete CDS of each hit was obtained. For the SDH3 subunit, mitochondrial sequences from several angiosperms were included for phylogenetic analysis given that this gene is variably encoded in the mitochondrial or the nuclear genome across angiosperms (Adams et al., 2001).

Nucleotide sequences of genes were aligned using MAFFT v.7.407 (parameters: --adjustdirectionaccurately --localpair --maxiterate 1000) (Katoh and Standley, 2013). Poorly aligned regions were removed with BMGE v.1.12 (parameters: --t DNA --m DNAPAM150:2) (Criscuolo and Gribaldo, 2010). Maximum Likelihood phylogenetic analyses were run with RAxML v.8.2.11 (Stamatakis, 2014) using the GTRGAMMA model and including 1,000 rapid bootstrap replicates. Trees

were visualized with FigTree v.1.4.4. Besides, to record the number of differences between native sequences in *Lophophytum* and mimosoid legume sequences, we compared the nuclear and mitochondrial encoded native genes in *Lophophytum* with those of mimosoid legumes based on the OXPHOS nucleotide alignments.

The information of the presence, membrane location, and phylogenetic origin of the products of mitochondrial and nuclear-encoded genes was illustrated in a schematic drawing of the OXPHOS and ccm system of *Lophophytum*. The schemes were adapted from KEGG (Kyoto Encyclopedia of Genes and Genomes) reference pathways (Kanehisa et al., 2021) and from *Arabidopsis* complex I (Ligas et al., 2019), complex II (Braun, 2020), complex III (Meyer et al., 2019), complex V (Röhricht et al., 2021), alternative respiratory pathways and ccm system (Hamel et al., 2009), and from *Vigna* complex IV (Maldonado et al., 2021).

2.3. Evolutionary analyses

Non-synonymous (dN) and synonymous (dS) substitution rates were estimated from individual alignments of protein-coding genes. The codeml program within PAML v.4.9 (Yang, 2007) was used to calculate the values of dN (the average number of non-synonymous differences for each non-synonymous site) and dS (the average number of synonymous differences for each synonymous site) based on each nucleotide alignment and gene phylogeny. It was assumed that all the branches have different dN and dS values (model = 1). The dN/dS ratio makes it possible to infer the selection pressure for each gene. A low ratio (dN/dS < 1) indicates purifying selection, a high ratio (dN/dS > 1) indicates positive selection, while a ratio close to 1 suggests the absence of natural selection and that the gene is evolving neutrally by genetic drift (Nielsen, 2005).

3. RESULTS

3.1. Evidence of a complete and functional OXPHOS and ccm system in *Lophophytum*

The plant mitochondrial OXPHOS is composed of five classic multiprotein complexes: NADH dehydrogenase (complex I), succinate dehydrogenase (complex II), cytochrome c reductase (complex III), cytochrome c oxidase (complex IV), and ATP synthase (complex V) (Braun, 2020; Meyer et al., 2019). Electrons enter the electron transport chain (ETC) of OXPHOS (complex I to IV) until the reduction of oxygen to water. The synthesis of ATP is carried out in complex V from the electrochemical gradient generated by the translocation of protons in complexes I, III, and IV. Homologs of the *Arabidopsis* nuclear genes that encode OXPHOS proteins were identified in the *Lophophytum* transcriptome through BLASTn and tBLASTn searches. Out of 71 nuclear-encoded subunits described in the five OXPHOS complexes of *Arabidopsis* (Meyer et al., 2019), homologs for all but two subunits were identified in the transcriptome of *Lophophytum* (Table 1). In all cases, the ORF lengths of the transcripts of *Lophophytum* were comparable to those in *Arabidopsis* and resemble mature RNAs (Table 1). The missing subunits correspond to complexes I (γ carbonic anhydrase subunit 3 - CA3) and II (SDH8). In *Arabidopsis*, the γ carbonic anhydrase domain is a trimer that can present the following conformations: CA2 + CA2 + CA-like, CA1 + CA1 + CA-like or homotrimer of CA3 (Córdoba et al., 2019). Nevertheless, the CA2-dependent trimer is the most abundant (80%) in adult plants and it has been suggested that CA3 might not be a subunit of complex I (Klodmann et al., 2010) but may play a role in the assembly and stabilization of complex I (Córdoba et al., 2019). In *Lophophytum*, one homolog to the pair of homologous genes CA1/2 of *Arabidopsis* and a homolog of the CA-like genes were identified (Table 1, Figure S1). Therefore, the γCA domain of *Lophophytum*

could exhibit different functional conformations, such as those described in *Arabidopsis*. The other homolog missing in *Lophophytum* is that encoding the SDH8 (At2g46390) subunit of complex II. Homologs of SDH8 have only been identified in the genomes of the family Brassicaceae and in monocots and it may not represent a true subunit of complex II (Schikowsky et al., 2017), although it might be more widely present but the small size makes its identification challenging (Huang et al., 2019). Homologs to all nuclear-encoded genes in *Arabidopsis* are also nuclear-encoded in *Lophophytum,* except for *sdh4* (complex II) that is mitochondrial-encoded in the holoparasite (Sanchez-Puerta et al., 2017). The genes *sdh3* and *sdh4* are encoded in the mtDNA of various plant species, while in others these genes have been functionally transferred to the nucleus (Adams et al., 2001). Overall, the set of OXPHOS subunits encoded in the *Lophophytum* nuclear genome is virtually complete, exhibiting over 97% of the subunits that make up the five OXPHOS complexes of *Arabidopsis*.

Cytochrome c is in charge of transporting electrons between complexes III and IV and it is encoded by nuclear genes in angiosperms. Two full-length homologs to cytochrome c were found in the *Lophophytum* transcriptome (Table 1). In *Arabidopsis*, the maturation system of type c cytochromes (ccm system) is carried out by proteins encoded in the mitochondrial (*ccmB*, *ccmC*, *ccmFN*, and *ccmFc*) or nuclear (*ccmA*, *ccmE,* and *ccmH*) genomes (Meyer et al., 2019; Rayapuram et al., 2007). In this work, homologs of the three nuclear genes were identified in the *Lophophytum* transcriptome, and the four mitochondrial-encoded genes were previously described in the *Lophophytum* mtDNA (Sanchez-Puerta et al., 2017).

In addition to the evidence provided by the presence of nearly all the genes (and of the expected length) for the assembly of OXPHOS and the ccm system in *Lophophytum*, the functionality was further evaluated by analyzing whether these genes are subject to evolutionary constraints. For each of the nuclear-encoded genes of *Lophophytum*, the selection pressure was assessed by estimating the dN/dS ratios. The dN/dS values were always far below 1 (Table 1), indicating that these genes are evolving under purifying selection. The mitochondrial-encoded genes were also shown to be evolving under selection pressure (Sanchez-Puerta et al., 2017). These results support a functional role of the OXPHOS in *Lophophytum*.

Table 1. Nuclear genes involved in OXPHOS, ccm system, and alternative respiratory pathways in *Arabidopsis* and *Lophophytum mirabile*. Shown are the ORF lengths and estimated ratios of synonymous (dS) and non-synonymous (dN) substitution rates (ω = dN/dS) of the nuclear genes of *Lophophytum*.

Multisubunit complex	**Subunit** [a]	***Arabidopsis* gene identifier** [b]	***Arabidopsis* ORF length (amino acids)**	***Lophophytum* assembled transcripts** [c]	***Lophophytum* ORF length (amino acids)**	**dN** [d]	**dS** [d]	**ω = dN/dS** [d]
OXPHOS Complex I	AGGG	At1g76200	69	TRINITY_DN8385_c0_g1_i11	84	0.048	1.033	0.046
	ASHI	At5g47570	125	TRINITY_DN4697_c0_g1_i2	126	0.105	1.061	0.099
	B8	At5g47890	97	TRINITY_DN4786_c0_g1_i3	98	0.113	1.031	0.109
	B9	At2g46540	65	TRINITY_DN6763_c0_g1_i2	70	0.219	0.66	0.332

B12	At2g02510/At1g14450	72/73	TRINITY_DN48247_c0_g1_i1	70	0.093	3241	0.029
B13	At5g52840	169	TRINITY_DN3373_c0_g1_i1	171	0.086	1.893	0.045
B14	At3g12260	133	TRINITY_DN16758_c0_g1_i1	132	0.141	1.752	0.081
B14.5a	At5g08060	131	TRINITY_DN25065_c0_g1_i2	130	0.132	0.504	0.262
B14.5b	At4g20150	81	TRINITY_DN3440_c0_g1_i9	80	0.052	0.947	0.056
B14.7	At2g42210	159	TRINITY_DN6377_c0_g2_i2	174	0.118	1.06	0.111
B15	At2g31490	71	TRINITY_DN6124_c0_g1_i1	71	0.091	2.606	0.035
B16.6	At2g33220/At1g04630	174/143	TRINITY_DN88_c0_g1_i1	143	0.073	1.466	0.05
B17.2	At3g03100	159	TRINITY_DN3824_c0_g1_i1	157	0.091	1.219	0.075
B18	At2g02050	103	TRINITY_DN67103_c0_g2_i1	103	0.088	1.871	0.047
B22	At4g34700	117	TRINITY_DN2483_c0_g1_i4	115	0.09	8.257	0.011
ESSS	At2g42310/At3g57785	114/114	TRINITY_DN482151_c0_g1_i1	115	0.114	1.97	0.058
MWFE	At3g08610	65	TRINITY_DN2895_c0_g2_i3	66	0.053	0.886	0.06
NDU10	At4g00585	88	TRINITY_DN10711_c0_g1_i5	85	0.168	1.025	0.164
PDSW	At1g49140/At3g18410	107/106	TRINITY_DN5599_c0_g1_i1	103	0.054	0.674	0.08
PGIV	At3g06310/At5g18800	108/106	TRINITY_DN39478_c0_g1_i12	106	0.068	1.722	0.039
PSST	At5g11770	218	TRINITY_DN7893_c0_g2_i2	209	0.004	0.05	0.071
P1	At1g67350	98	TRINITY_DN176_c0_g1_i1	90	0.199	0.526	0.378
P2	At2g27730	113	TRINITY_DN11135_c1_g2_i1	116	0.113	2.173	0.052
P4	At1g67785	63	TRINITY_DN40371_c0_g4_i1	62	0.132	0.674	0.195
TYKY	At1g79010/At1g16700	222/222	TRINITY_DN2693_c0_g1_i2	224	0.066	0.66	0.1
γ Carbonic anhydrase 1/2	At1g19580/At1g47260	275/278	TRINITY_DN17286_c2_g4_i1	276	0.038	0.843	0.045
γ Carbonic anhydrase 3	At5g66510	258	–	–	–	–	–
γ Carbonic anhydrase like	At3g48680/At5g63510	256/252	TRINITY_DN13205_c0_g1_i1	247	0.073	2.382	0.031
13 kDa	At3g03070	110	TRINITY_DN305_c0_g1_i6	114	0.113	1.952	0.058
15 kDa	At3g62790/ At2g47690	83/118	TRINITY_DN6660_c0_g1_i1	84	0.138	1.605	0.086
18 kDa	At5g67590	154	TRINITY_DN3153_c0_g1_i9	154	0.065	1.151	0.057
20.9 kDa	At4g16450	106	TRINITY_DN553_c0_g1_i1	100	0.052	1.51	0.035
24 kDa	At4g02580	255	TRINITY_DN2804_c0_g1_i3	254	0.069	1.148	0.06

	39 kDa	At2g20360	402	TRINITY_DN3051_c0_g1_i4	408	0.092	1.342	0.068
	51 kDa	At5g08530	486	TRINITY_DN43587_c0_g4_i1	484	0.02	1.859	0.01
	75 kDa	At5g37510	745	TRINITY_DN17151_c0_g1_i1	751	0.08	2.214	0.036
OXPHOS Complex II	SDH1	At5g66760/At2g18450	634/632	TRINITY_DN2934_c0_g1_i1	632	0.006	1.437	0.004
	SDH2	At3g27380/At5g40650/At5g65165	279/280/309	TRINITY_DN485144_c0_g1_i1	280	0.048	1.688	0.029
	SDH3	**At4g32210/At5g09600**	**213/213**	**TRINITY_DN2695_c0_g2_i1**	**250**	**0.066**	**0.295**	**0.223**
	SDH4	**At2g46505**	**151**	**Mitochondrial genome (GenBank: KU992331.1)**	**128**	**—**	**—**	**—**
	SDH5	At1g47420	257	TRINITY_DN5481_c0_g1_i1	258	0.127	1.66	0.077
	SDH6	At1g08480	142	TRINITY_DN36101_c0_g1_i6	149	0.137	1.007	0.136
	SDH7	At3g47833/At5g62575	93/100	TRINITY_DN7006_c0_g2_i12	107	0.119	2.044	0.059
	SDH8	At2g46390	46	—	—	—	—	—
OXPHOS Complex III	CYC1	At5g40810/At3g27240	307/307	TRINITY_DN5853_c0_g1_i3	364	0.052	1.102	0.047
	MPPα	At1g51980/At3g16480	503/499	TRINITY_DN7699_c0_g1_i8	506	0.125	1.092	0.114
	MPPβ	At3g02090	531	TRINITY_DN1744_c0_g1_i3	525	0.079	2.247	0.035
	QCR6	At1g15120/At2g01090	69/62	TRINITY_DN1011_c0_g1_i12	103	0.145	0.435	0.333
	QCR7	At4g32470/At5g25450	101/122	TRINITY_DN949_c0_g2_i3	124	0.096	2.171	0.044
	QCR9	At3g52730	72	TRINITY_DN5505_c0_g1_i1	72	0.255	1.404	0.181
	UCRQ	At3g10860/At5g05370	72/72	TRINITY_DN2665_c0_g1_i1	74	0.136	1.002	0.136
	UCRY	At2g40765	57	TRINITY_DN4637_c0_g1_i3	61	0.13	0.909	0.143
	UCR1	At5g13430/At5g13440	272/274	TRINITY_DN8828_c0_g1_i1	275	0.079	1.3	0.061
OXPHOS Complex IV	COX-X1	At5g27760	96	TRINITY_DN5832_c0_g1_i1	98	0.04	1.505	0.027
	COX-X2	At4g00860/At1g01170	80/83	TRINITY_DN4992_c0_g1_i2	79	0.131	0.836	0.156
	COX-X3	At1g72020	97	TRINITY_DN1126_c0_g3_i1	95	0.165	0.579	0.286
	COX-X4	At4g21105	68	TRINITY_DN3581_c2_g1_i2	67	0.087	0.814	0.107
	COX5b	At3g15640/At1g80230/At1g52710	176/171/90	TRINITY_DN5962_c0_g1_i3	156	0.051	6.133	0.008
	COX5c	At2g47380/At5g40382/At5g61310	64/64/64	TRINITY_DN2941_c0_g2_i1	63	0.082	2.831	0.029
	COX6a	At4g37830	102	TRINITY_DN1379_c0_g1_i4	98	0.23	1.301	0.177
	COX6b	At1g22450	222/222	TRINITY_DN7733_c0_g1_i3	221	0.038	1.032	0.037
		At5g57815/At4g28060	78/ 78	TRINITY_DN2697_c0_g2_i2	76	0.105	1.277	0.082
OXPHOS Complex V	ATP-FAD	At2g21870	240	TRINITY_DN2772_c0_g1_i1	235	0.131	1.407	0.093
	ATP2	At5g08670/At5g08680/At5g08690	556/559/556	TRINITY_DN10090_c1_g1_i3	557	0.021	1.164	0.018

	ATP3	At2g33040	325	TRINITY_DN6198_c0_g2_i1	322	0.088	0.83	0.106
	ATP5	At5g13450	238	TRINITY_DN92821_c0_g1_i1	253	0.129	0.871	0.149
	ATP 6kDa	At3g46430/At5g59613	55/55	TRINITY_DN11276_c0_g1_i4	55	0.03	0.968	0.098
	ATP7	At3g52300	168	TRINITY_DN3804_c0_g1_i2	168	0.074	1.612	0.046
	ATP15	At1g51650	70	TRINITY_DN369_c0_g1_i1	68	0.21	1.742	0.121
	ATP16	At5g47030	203	TRINITY_DN2618_c0_g1_i1	204	0.083	1.392	0.059
	ATP17	At4g30010	90	TRINITY_DN1768_c0_g1_i1	90	0.142	0.843	0.169
	ATP20	At4g29480/At2g19680/At4g26210	122/122/122	TRINITY_DN5010_c0_g1_i1	122	0.05	0.462	0.108
				TRINITY_DN337980_c0_g1_i1	122	0.098	0.4	0.246
Alternative oxidases	AOX1	At3g22370/At3g22360/At3g27620/At1g32350	354/325/329/318	TRINITY_DN1828_c0_g1_i2	297	0.048	0.892	0.054
				TRINITY_DN4169_c1_g1_i5	283	0.031	0.584	0.056
	AOX2	At5g64210	353	TRINITY_DN10127_c0_g1_i1	326	0.05	0.546	0.092
Alternative NADH dehydrogenases	NDA1/NDA2	At1g07180/At2g29990	510/508	TRINITY_DN10736_c2_g2_i2	502	0.066	1.019	0.064
		–	–	TRINITY_DN2383_c0_g1_i1	539	0.047	1.482	0.031
	NDB1	At4g28220	571	–	–	–	–	–
	NDB2/NDB3	At4g05020/At4g21490	582/580	TRINITY_DN10_c1_g3_i1	581	0.049	1.437	0.034
	NDB4	At2g20800	582	–	–	–	–	–
	NDC	At5g08740	519	–	–	–	–	–
Ccm system	CcmA	At1g63270	229	TRINITY_DN405679_c0_g1_i1	229	0.052	1.1	0.047
	CcmE	At3g51790	256	TRINITY_DN264122_c0_g1_i1	256	0.066	1.528	0.043
	CcmH	At1g15220	159	TRINITY_DN2969_c0_g1_i5	169	0.068	2.277	0.03
Cytochrome c	Cytc-1/Cytc-2	At4g10040/At1g22840	112/114	TRINITY_DN2556_c0_g2_i1	112	0.07	0.605	0.115
				TRINITY_DN95492_c0_g3_i1	113	0.173	0.517	0.335

a Boldfaced names indicate that the homologous genes in *Lophophytum* are foreign.

b A dash indicates a missing gene copy in *Arabidopsis* but present in *Lophophytum*.

c A dash indicates that the *Arabidopsis* homolog is absent in the *Lophophytum* transcriptome.

d The PAML V.4.9 program (http://abacus.gene.ucl.ac.uk/software/paml.html) (Yang, 2007) was used to estimate dN and dS under the model = 1 of codeml.

3.2. All but one of the nuclear-encoded genes of the OXPHOS and ccm system are native in *Lophophytum*

Phylogenetic analyses of each of the nuclear-encoded subunits in *Lophophytum* revealed that all but one are native (Figure S1). Given the lack of nuclear sequences from Santalales, homologs of *Lophophytum* that are found in different locations in the phylogenetic trees, but not associated with the Fabaceae family with high bootstrap support (≥70%) were conservatively considered native. The

expected phylogenetic position of vertically-inherited genes of *Lophophytum* is sister to asterids (Li et al., 2019; The Angiosperm Phylogeny Group et al., 2016) or to rosids (Leebens-Mack et al., 2019). For example, Figure 1 shows the phylogeny of the SDH1 subunit of OXPHOS complex II. This phylogenetic tree shows that the homolog of *Lophophytum* is distant from the clade that represents the Fabaceae suggesting its native origin. In contrast, Figure 2 shows the phylogeny of the SDH3 subunit of OXPHOS complex II, which is mitochondrial or nuclear-encoded across angiosperms due to multiple independent intracellular functional transfers from the mitochondrial to the nuclear genome (Adams et al., 2001). The sequence corresponding to *Lophophytum* is nuclear-encoded and related to that of *Prosopis alba* (Fabaceae, mimosoid clade) with strong bootstrap support (94%), indicating that this gene is foreign in *Lophophytum* and it was acquired via HGT from a mimosoid legume host. Detailed sequence analyses indicated that the transit peptide is also similar to that of *Prosopis* evidencing a nucleus-to-nucleus horizontal transfer of the *sdh3* (Garcia et al., 2021). The remaining phylogenetic trees (Figure S1) indicate a native origin for all the homologs of *Lophophytum* involved in OXPHOS and ccm system. In a few cases, more than one homolog were identified in *Lophophytum*, which are the result of ancestral (COX6b) or more recent (ATP20, cytc) gene duplications, as also observed in other angiosperms.

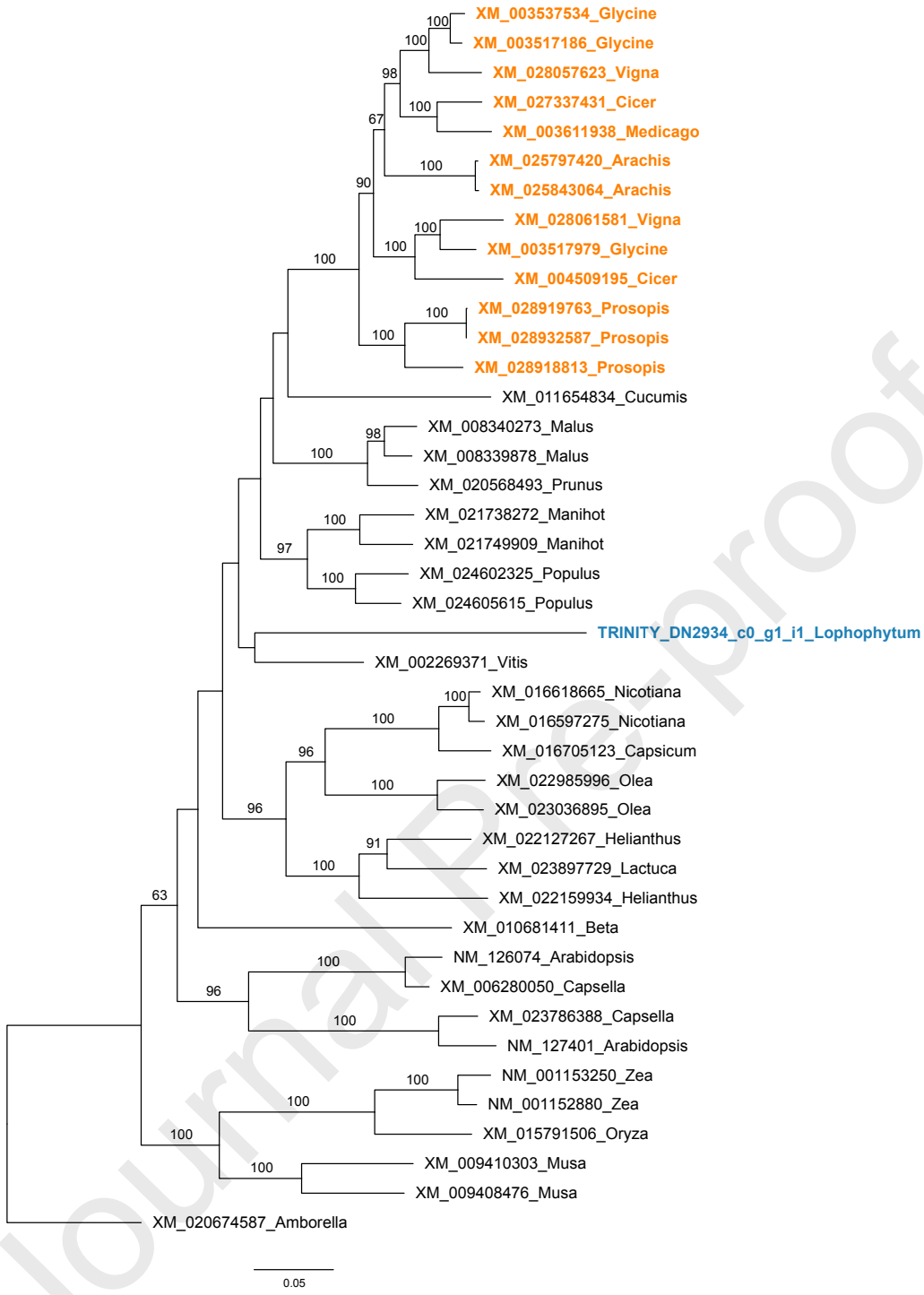

Figure 1. Example of a native nuclear-encoded gene in *Lophophytum mirabile*. Maximum Likelihood (ML) phylogenetic analysis of the gene for the SDH1 subunit present in complex II of OXPHOS. ML bootstrap support values ≥50% from 1,000 bootstrap replicates are shown above each branch. The scale bar corresponds to substitutions per site. *Lophophytum* and Fabaceae sequences are in blue and orange, respectively.

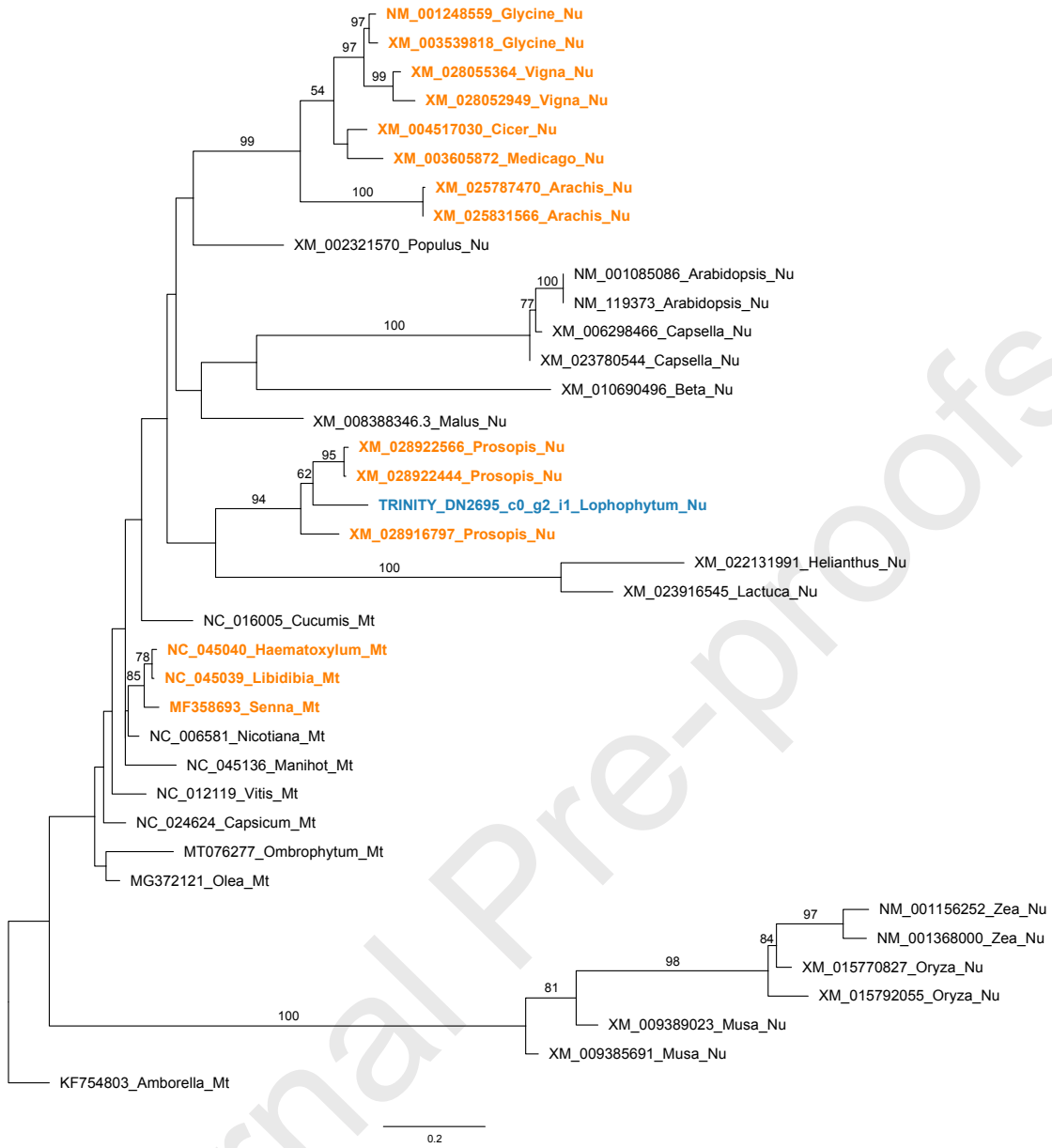

Figure 2. Example of a foreign nuclear-encoded gene in *Lophophytum mirabile*. Maximum likelihood (ML) phylogenetic analysis of the gene for the SDH3 subunit present in the complex II of the OXPHOS. ML bootstrap support values ≥50% from 1,000 bootstrap replicates are shown above each branch. The scale bar corresponds to substitutions per site. *Lophophytum* and Fabaceae sequences are in blue and orange, respectively. Mt: mitochondrial-encoded genes; Nu: nuclear-encoded genes.

3.3. Alternative respiratory pathways in *Lophophytum*

Besides the five classic protein complexes, plant OXPHOS present alternative pathways to electron flow: nuclear-encoded alternative oxidases (AOX) and alternative NADH dehydrogenases (altND) (Meyer et al., 2019). Electrons may enter through an altND and be transferred to AOX for oxygen reduction, without proton translocation (Millar et al., 2011). Alternatively, electrons inserted into altNDs can be coupled to proton translocation in complexes III and IV, while electrons entered into

complex I can be transported to AOXs for oxygen reduction (Braun, 2020). Homologs for most of the altND and AOX described in *Arabidopsis* were found in *Lophophytum* (Table 1). Two and one homologs to the *Arabidopsis* genes AOX1 and AOX2, respectively, were identified in the *Lophophytum* transcriptome (Table 1). Regarding the altND, seven subunits make up this complex in *Arabidopsis*, four located externally (NDB1, NDB2, NDB3, and NDB4) and three internally (NDA1, NDA2, and NDC) in the inner part of the inner membrane of the mitochondria (Braun, 2020). Homologs to NDB1, NDB4, and NDC were not identified in the *Lophophytum* transcriptome. Nevertheless, of the four altNDs located externally, the NDB2 is the predominant external NADH dehydrogenase in *Arabidopsis* mitochondria (Sweetman et al., 2019). NDC is also targeted to the chloroplast and participates in plastoquinone reduction and phylloquinone biosynthesis (Piller et al., 2011). Noticeably, NDC transcripts are also missing in holoparasitic plants of the family Orobanchaceae (Gu et al., 2021). All genes involved in the alternative respiratory pathways in *Lophophytum* are nuclear-encoded and evolving under purifying selection (Table 1), providing indirect evidence of their functional status. Phylogenetic trees showed that all homologs of the altND and AOX are native in *Lophophytum* with a recent duplication of the AOX1 gene (Figure S1).

4. DISCUSSION

4.1. The mosaic OXPHOS of *Lophophytum* highly resembles that of free-living angiosperms but may be less efficient

Several lines of evidence provided here and in earlier studies (Garcia et al., 2021; Sanchez-Puerta et al., 2017) indicate that the OXPHOS in *Lophophytum* is similar to that of free-living plants and is likely functional: i) the mtDNA gene content includes all the expected genes coding for OXPHOS subunits; ii) mitochondrial-encoded OXPHOS genes are efficiently expressed, edited, and spliced; iii) homologs for nearly all nuclear genes coding for OXPHOS subunits in the *Arabidopsis* nuclear genome were identified in the transcriptome of *Lophophytum* and show the expected length; and iv) mitochondrial and nuclear-encoded OXPHOS genes are evolving under strong purifying selection.

However, *Lophophytum* exhibits an unexpected situation in its mitochondria given that eleven OXPHOS and three ccm system subunits encoded in the mitochondrial genome are completely or partially foreign, while eight OXPHOS and one ccm system mitochondrial-encoded subunits are native (Garcia et al., 2021; Sanchez-Puerta et al., 2017). Furthermore, all but one (SDH3) nuclear-encoded subunits are native. As a result, the OXPHOS complex III is the only one with mitochondrial and nuclear subunits that are entirely native. In contrast, the OXPHOS complexes I, II, IV, and V are made up of native and foreign (or chimeric) mitochondrial proteins and native nuclear proteins, except for the foreign nuclear *sdh3* in complex II (Figure 3). In addition, the foreign and native subunits of *Lophophytum* have a wider range of interactions given that the OXPHOS complexes can be found forming supercomplexes (Eubel et al., 2004; Schägger and Pfeiffer, 2000; Ukolova et al., 2020). Likewise, the mitochondrial genes *ccmB*, *ccmC,* and *ccmFc* are foreign in *Lophophytum* (Garcia et al., 2021; Sanchez-Puerta et al., 2017), while *ccmFN* and the nuclear genes (*ccmA*, *ccmE,* and *ccmH*) are native, evidencing the mosaic nature of the ccm system (Figure 3). Overall, the OXPHOS and ccm system in *Lophophytum* consist of a mosaic of mitochondrial and nuclear subunits with different phylogenetic origin (Figure 3), a situation that might generate conflicts in the interactions among mitochondrial proteins and also, nuclear cytoplasmic incompatibilities.

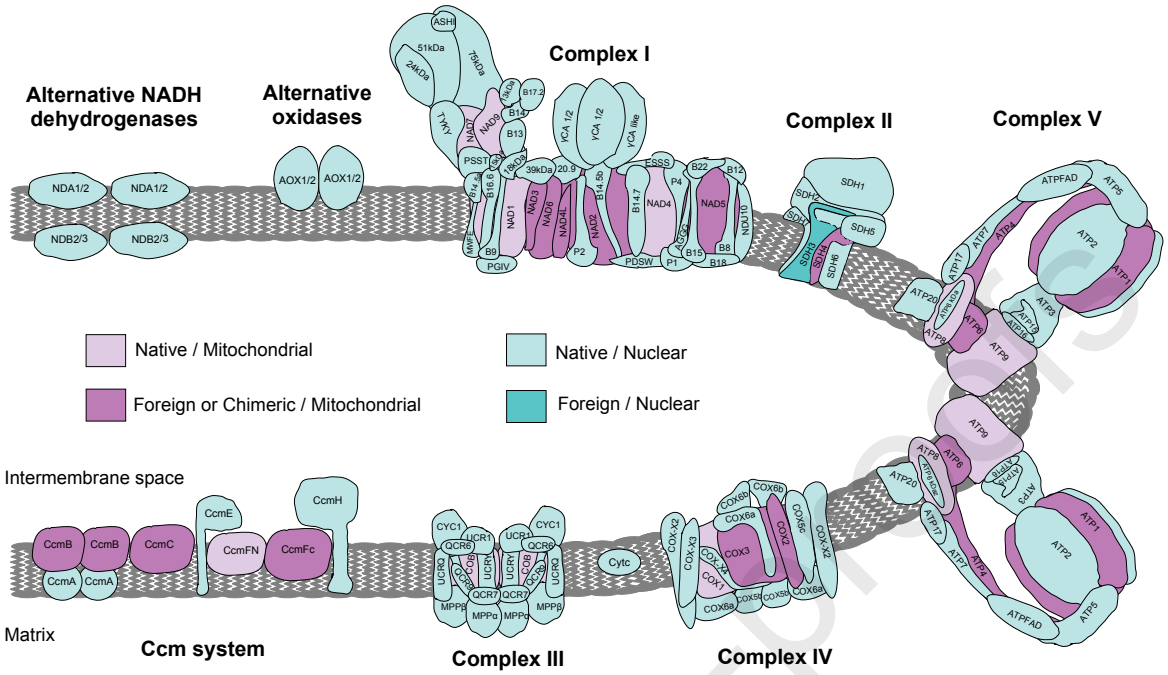

Figure 3. Schematic structure of the mosaic OXPHOS and ccm system in the inner mitochondrial membrane of *Lophophytum*, as well as that of the alternative respiratory pathways. Nuclear encoded genes are shown in light and dark indigo if native or foreign, respectively. Mitochondrial encoded genes are shown in light and dark purple if native or foreign/chimeric, respectively. The association of the plant-specific subunit COX1-X1 within complex IV is still unclear and is not shown.

Nuclear and mitochondrial genes whose products interact in multiprotein complexes are known to co-evolve over time. The co-evolution of cytonuclear enzyme complexes implies that rapid changes (or replacements) of one of the co-adapted genes could cause incompatibilities that lead to fitness reduction, generating a selection pressure for subsequent changes in genes in the other genome. In fact, plants with high substitution rates in their plastid and/or mitochondrial genomes show an increase in the evolutionary rates of nuclear genes whose products interact with organellar-encoded proteins within the organellar compartments (Rockenbach et al., 2016; Sloan et al., 2014; Weng et al., 2016; Williams et al., 2019; Zhang et al., 2015). In some cases, rapid changes can disrupt a metabolic pathway. A few *Silene* species with high rates of substitutions in their mitochondrial genes (Havird et al., 2019) exhibit a decrease in respiratory efficiency relying more heavily on alternative oxidases and accessory dehydrogenases (Weaver et al., 2020). Severe phenotypes, such as cytoplasmic male sterility (CMS), have been described when the mitochondrial gene content is impacted by interspecific plant hybridization events creating cytonuclear incompatibilities, even between closely related species (Chase, 2007; Sabar et al., 2000; Touzet and Meyer, 2014). Similarly, the massive mitochondrial HGT from the distantly related host plants to *Lophophytum* and the functional substitution of several mitochondrial-encoded genes that have evolved interacting with a different nuclear background opens

the possibility of incompatibilities within OXPHOS complexes or the ccm system that may affect the respiration rate and efficiency of the holoparasite.

4.2. The unexpected functional acquisition of foreign subunits that form part of multisubunit complexes in *Lophophytum*

It is puzzling that foreign mitochondrial genes, such as those encoding OXPHOS subunits, reached fixation even when their products likely disrupt the interactions between co-evolved native proteins within multisubunit complexes. A possible explanation involves the role of genetic drift. After the fortuitous acquisition of foreign genes, some of them could have been fixed by chance, instead of being eliminated by natural selection based on the negative physiological effect on cellular respiration (e.g. a decrease in ATP production). Genetic drift plays an important role in organisms with small populations, as inferred for *Lophophytum* (Garcia et al., 2021), leading to an evolutionary situation that may be slightly unfavorable from the energetic standpoint, but still viable. In this case, the foreign mitochondrial genes could have been maintained by genetic drift even when producing a slightly deleterious effect. This effect could have been limited by the low substitution rates of angiosperm mitochondrial genomes (Bellot et al., 2016; Drouin et al., 2008; Palmer and Herbon, 1988; Zervas et al., 2019). Thus, the foreign mitochondrial protein-coding genes donated by the Fabaceae would be translated into proteins that resemble the native ones creating minor incompatibilities in the assembly and function of the OXPHOS. Likewise, genes transferred between closely related bacteria do not interfere with the functioning of protein complexes because they are very similar to the native ones (Soucy et al., 2015; Tian et al., 2015). A negative correlation has been observed between the number of HGT events and the evolutionary distance of donor and recipient bacterial species (Williams et al., 2012). Therefore, given the low divergence between the Fabaceae and *Lophophytum* mitochondrial proteins, the functional substitution of several native OXPHOS genes by mimosoid homologs could have occurred by genetic drift leading to a slightly lower respiratory efficiency and increased dependence on alternative pathways of the electron transport chain, but these aspects remain unexplored. This putative decrease in fitness was likely mitigated by the parasitic lifestyle, slow growth, and small size of *Lophophytum*. Future work should focus on experimentally evaluating the ATP production and oxygen consumption in the presence of ADP or specific electron donors and inhibitors. Comparing the respiration efficiency in *Lophophytum* and in the closely related holoparasite *Ombrophytum subterraneum* that maintains native mitochondrial genes for each of the OXPHOS complexes (Roulet et al., 2020) would be valuable to further understand the impact of HGT in this holoparasitic plant.

In contrast to mitochondrial genes, nuclear genes among angiosperms display higher rates of substitution (Drouin et al., 2008). The native nuclear proteins of *Lophophytum* are more divergent with respect to the nuclear proteins of the Fabaceae in comparison to their mitochondrial proteins. Thus, a replacement of a native nuclear gene by a host-derived homolog would likely create strong incompatibilities in the interactions with native subunits within the OXPHOS complexes or the ccm system. Comparisons of several nuclear genes involved in OXPHOS exhibit 54-83% similarity between the protein sequences of *Lophophytum* and the mimosoid legume *Prosopis*. The acquisition of a foreign nuclear gene that interacts with native subunits of OXPHOS would have likely resulted in a severe drop in fitness, followed by the evolutionary loss of such foreign homolog by natural selection. This scenario is largely compatible with the phylogenetic results, in which all but one of the nuclear-encoded genes involved in multisubunit complexes are native in *Lophophytum*. Nevertheless, this study represents a first glimpse of the impact of HGT in the nucleus of the holoparasite. It is also possible that the level of nucleus-to-nucleus transfer events between *Lophophytum* and its host is low and many of the OXPHOS nuclear genes have never been acquired by the holoparasite. However, the genome-scale horizontal transfers of mitochondrial DNA to the *Lophophytum* mtDNA (Sanchez-Puerta et al., 2017) suggest that

nuclear DNA from the host plants has also been transferred to the holoparasite nuclear genome. Genome-wide analyses will reveal to what extent the nuclear genome of *Lophophytum* was shaped by HGT and if other cytonuclear complexes (e.g. mitochondrial ribosomes) show similar evolutionary patterns.

4.3. Co-acquisition of *sdh4* and *sdh3* as a result of cooperation between foreign genes?

It has been proposed that the accidental acquisition of a foreign nuclear gene that interacts with other foreign subunits of OXPHOS could have been retained by natural selection as they might represent a fitness increase by minimizing the incompatibilities in the assembly and functioning of these multiprotein complexes. An example of this scenario could be the co-acquisition of the mitochondrial *sdh4* and the nuclear *sdh3* from mimosoid hosts.

In contrast to the 25 core mitochondrial genes almost universally present across angiosperms (Mower et al., 2012), ribosomal protein genes and those encoding subunits of OXPHOS complex II (*sdh3*, *sdh4*) are variably present in the mitochondrial genomes of flowering plants (Adams et al., 2002). In at least 14 and eight independent events across angiosperms, the genes *sdh3* and *sdh4*, were functionally transferred to the nuclear genome, respectively (Liu et al., 2009). Both genes are nuclear-encoded in *Arabidopsis*, while *sdh3* is nuclear-encoded and *sdh4* is mitochondrial-encoded in mimosoid legumes (Adams et al., 2001; Choi et al., 2019). In the family Balanophoraceae, the genes *sdh3* and *sdh4* are located in the mtDNA of *Ombrophytum* (Roulet et al., 2020), *Rhopalocnemis,* and *Balanophora* (Renchao Zhou pers. comm.). Similarly, the *sdh4* is located in the mtDNA of *Lophophytum* although a foreign copy has replaced the native homolog (Sanchez-Puerta et al., 2017). Noticeably, the native *sdh3* has been functionally replaced in *Lophophytum* by a nuclear-encoded mitochondrial-targeted *sdh3* acquired from the legume hosts. For some time, both the native and the foreign *sdh3* must have co-existed and been functional in the mitochondria, until the native *sdh3* became a pseudogene. The foreign SDH3 protein is likely quite different from the native protein, based on present-day comparisons. At the amino acid level, *Ombrophytum* mitochondrial-encoded *sdh3* (resembling the native *sdh3*) is 54% similar to the nuclear-encoded *sdh3* of *Prosopis* (resembling the foreign *sdh3*). The retention of the nuclear foreign copy over the native one could have been driven by the functional replacement of the mitochondrial gene *sdh4* by a host-derived copy, or vice versa. Complex II is composed of four classical subunits, of which the membrane subunits SDH3 and SDH4 anchor the two catalytic subunits, SDH1 and SDH2 (Braun, 2020; Huang et al., 2019; Meyer et al., 2019). The proteins SDH3 and SDH4 are inserted in the inner mitochondrial membrane and exhibit extensive physical contact with each other (Sun et al., 2005). Cooperation between two foreign genes from the same donor, such as *sdh3* and *sdh4*, can result in gene co-occurrence in the recipient organism. Individually, each foreign gene may have caused deleterious effects but together they may have resulted in a benefit of cell fitness (Hall et al., 2020). Foreign genes may be acquired simultaneously or sequentially, similar to the mitonuclear co-introgression of mtDNA and nuclear-encoded mitochondrial-targeted genes observed in hybrids, which would attenuate the effects of breaking up co-evolved mitochondrial and nuclear genes (Burton et al., 2013).

ACKNOWLEDGMENTS

We thank Renchao Zhou for sharing unpublished results, Elina Welchen for fruitful discussions, and M. Emilia Roulet for critically reading this manuscript.

FUNDING

This work used the Toko Cluster from FCEN-UNCuyo, which is part of the SNCAD-MinCyT, Argentina. This work was supported by Agencia Nacional de Promoción Científica y Tecnológica (PICT-2017-0691) and Universidad Nacional de Cuyo (06/A724) through funding to M.V.S.P.

CREDIT AUTHOR STATEMENT

L. M. Gatica-Soria: Data Curation, Formal Analysis, Original Draft Preparation, Visualization. L. F. Ceriotti: Investigation, Writing, Reviewing and Editing. L. E. Garcia: Supervision, Writing, Reviewing and Editing. M.V. Sanchez-Puerta: Conceptualization, Supervision, Writing, Reviewing and Editing.

REFERENCES

Adams, K.L., Qiu, Y.L., Stoutemyer, M., Palmer, J.D., 2002. Punctuated evolution of mitochondrial gene content: High and variable rates of mitochondrial gene loss and transfer to the nucleus during angiosperm evolution. Proceedings of the National Academy of Sciences of the United States of America 99, 9905–9912.

Adams, K.L., Rosenblueth, M., Qiu, Y.L., Palmer, J.D., 2001. Multiple losses and transfers to the nucleus of two mitochondrial succinate dehydrogenase genes during angiosperm evolution. Genetics 158, 1289–1300.

Bellot, S., Cusimano, N., Luo, S., Sun, G., Zarre, S., Gröger, A., Temsch, E., Renner, S.S., 2016. Assembled Plastid and Mitochondrial Genomes, as well as Nuclear Genes, Place the Parasite Family Cynomoriaceae in the Saxifragales. Genome Biology and Evolution 8, 2214–2230.

Bolger, A.M., Lohse, M., Usadel, B., 2014. Trimmomatic: A flexible trimmer for Illumina sequence data. Bioinformatics 30, 2114–2120.

Braun, H.P., 2020. The Oxidative Phosphorylation system of the mitochondria in plants. Mitochondrion 53, 66–75.

Burton, R.S., Pereira, R.J., Barreto, F.S., 2013. Cytonuclear genomic interactions and hybrid breakdown. Annual Review of Ecology, Evolution, and Systematics 44, 281–302.

Ceriotti, L.F., Roulet, M.E., Sanchez-Puerta, M.V., 2021. Plastomes in the holoparasitic family Balanophoraceae: Extremely high AT content, severe gene content reduction, and two independent genetic code changes. Molecular Phylogenetics and Evolution 162, 107208.

Chase, C.D., 2007. Cytoplasmic male sterility: a window to the world of plant mitochondrial-nuclear interactions. Trends in Genetics 23, 81–90.

Choi, I.S., Schwarz, E.N., Ruhlman, T.A., Khiyami, M.A., Sabir, J.S.M., Hajarah, N.H., Sabir, M.J., Rabah, S.O., Jansen, R.K., 2019. Fluctuations in Fabaceae mitochondrial genome size and content are both ancient and recent. BMC Plant Biology 19, 448.

Córdoba, J.P., Fassolari, M., Marchetti, F., Soto, D., Pagnussat, G.C., Zabaleta, E., 2019. Different Types Domains are Present in Complex I from Immature Seeds and of CA Adult Plants in Arabidopsis thaliana. Plant and Cell Physiology 60, 986–998.

Criscuolo, A., Gribaldo, S., 2010. BMGE (Block Mapping and Gathering with Entropy): A new software for selection of phylogenetic informative regions from multiple sequence alignments. BMC Evolutionary Biology 10.

Drouin, G., Daoud, H., Xia, J., 2008. Relative rates of synonymous substitutions in the mitochondrial, chloroplast and nuclear genomes of seed plants. Molecular Phylogenetics and Evolution 49, 827–831.

Eubel, H., Heinemeyer, J., Braun, H.P., 2004. Identification and characterization of respirasomes in potato mitochondria. Plant Physiology 134, 1450–1459.

Garcia, L.E., Edera, A.A., Palmer, J.D., Sato, H., Sanchez-Puerta, M.V., 2021. Horizontal gene transfers dominate the functional mitochondrial gene space of a holoparasitic plant. New Phytologist 229, 1701–1714.

Grabherr, M.G., Haas, B.J., Yassour, M., Levin, J.Z., Thompson, D.A., Amit, I., Adiconis, X., Fan, L., Raychowdhury, R., Zeng, Q., Chen, Z., Mauceli, E., Hacohen, N., Gnirke, A., Rhind, N., Di Palma, F., Birren, B.W., Nusbaum, C., Lindblad-Toh, K., Friedman, N., Regev, A., 2011. Full-length transcriptome assembly from RNA-Seq data without a reference genome. Nature Biotechnology 29, 644–652.

Gu, X., Chen, I.G., Harding, S.A., Nyamdari, B., Ortega, M.A., Clermont, K., Westwood, J.H., Tsai, C.J., 2021. Plasma membrane phylloquinone biosynthesis in nonphotosynthetic parasitic plants. Plant Physiology 185, 1443–1456.

Gualberto, J.M., Newton, K.J., 2017. Plant Mitochondrial Genomes: Dynamics and Mechanisms of Mutation. Annual Review of Plant Biology 68, 225–252.

Hall, R.J., Whelan, F.J., McInerney, J.O., Ou, Y., Domingo-Sananes, M.R., 2020. Horizontal Gene Transfer as a Source of Conflict and Cooperation in Prokaryotes. Frontiers in Microbiology 11.

Hamel, P., Corvest, V., Giegé, P., Bonnard, G., 2009. Biochemical requirements for the maturation of mitochondrial c-type cytochromes. Biochimica et Biophysica Acta - Molecular Cell Research 1793, 125–138.

Hansen, B., 1980. Balanophoraceae. Flora Neotropica 23, 1–80.

Havird, J.C., Noe, G.R., Link, L., Torres, A., Logan, D.C., Sloan, D.B., Chicco, A.J., 2019. Do angiosperms with highly divergent mitochondrial genomes have altered mitochondrial function? Mitochondrion 49, 1–11.

Huang, S., Braun, H.P., Gawryluk, R.M.R., Millar, A.H., 2019. Mitochondrial complex II of plants: subunit composition, assembly, and function in respiration and signaling. Plant Journal 98, 405–417.

Kanehisa, M., Furumichi, M., Sato, Y., Ishiguro-Watanabe, M., Tanabe, M., 2021. KEGG: integrating viruses and cellular organisms. Nucleic Acids Research 49, D545–D551.

Katoh, K., Standley, D.M., 2013. MAFFT multiple sequence alignment software version 7: Improvements in performance and usability. Molecular Biology and Evolution 30, 772–780.

Klodmann, J., Sunderhaus, S., Nimtz, M., Jänsch, L., Braun, H.P., 2010. Internal architecture of mitochondrial complex I from Arabidopsis thaliana. Plant Cell 22, 797–810.

Leebens-Mack, J.H., Barker, M.S., Carpenter, E.J., Deyholos, M.K., Gitzendanner, M.A., Graham, S.W., Grosse, I., Li, Z., Melkonian, M., Mirarab, S., Porsch, M., Quint, M., Rensing, S.A., Soltis, D.E., Soltis, P.S., Stevenson, D.W., Ullrich, K.K., Wickett, N.J., DeGironimo, L., Edger, P.P., Jordon-Thaden, I.E., Joya, S., Liu, T., Melkonian, B., Miles, N.W., Pokorny, L., Quigley, C., Thomas, P., Villarreal, J.C., Augustin, M.M., Barrett, M.D., Baucom, R.S., Beerling, D.J., Benstein, R.M., Biffin, E., Brockington, S.F., Burge, D.O., Burris, J.N., Burris, K.P., Burtet-Sarramegna, V., Caicedo, A.L., Cannon, S.B., Çebi, Z., Chang, Y., Chater, C., Cheeseman, J.M., Chen, T., Clarke, N.D., Clayton, H., Covshoff, S., Crandall-Stotler, B.J., Cross, H., DePamphilis, C.W., Der, J.P., Determann, R., Dickson, R.C., Di Stilio, V.S., Ellis, S., Fast, E., Feja, N., Field, K.J., Filatov, D.A., Finnegan, P.M., Floyd, S.K., Fogliani, B., García, N., Gâteblé, G., Godden, G.T., Goh, F. (Qi Y., Greiner, S., Harkess, A., Heaney, J.M., Helliwell, K.E., Heyduk, K., Hibberd, J.M., Hodel, R.G.J., Hollingsworth, P.M., Johnson, M.T.J., Jost, R., Joyce, B., Kapralov, M.V., Kazamia, E., Kellogg, E.A., Koch, M.A., Von Konrat, M., Könyves, K., Kutchan, T.M., Lam, V., Larsson, A., Leitch, A.R., Lentz, R., Li, F.W., Lowe, A.J., Ludwig, M., Manos, P.S., Mavrodiev, E., McCormick, M.K., McKain, M., McLellan, T., McNeal, J.R., Miller, R.E., Nelson, M.N., Peng, Y., Ralph, P., Real, D., Riggins, C.W., Ruhsam, M., Sage, R.F., Sakai, A.K., Scascitella, M., Schilling, E.E., Schlösser, E.M., Sederoff, H., Servick, S., Sessa, E.B., Shaw, A.J., Shaw, S.W., Sigel, E.M., Skema, C., Smith, A.G., Smithson, A., Stewart, C.N., Stinchcombe, J.R., Szövényi, P., Tate, J.A., Tiebel, H., Trapnell, D., Villegente, M., Wang, C.N., Weller, S.G., Wenzel, M., Weststrand, S., Westwood, J.H., Whigham, D.F., Wu, S., Wulff, A.S., Yang, Y., Zhu, D., Zhuang, C., Zuidof, J., Chase, M.W., Pires, J.C., Rothfels, C.J., Yu, J., Chen, C., Chen, L., Cheng, S., Li, J., Li, R., Li, X., Lu, H., Ou, Y., Sun, X., Tan, X., Tang, J., Tian, Z., Wang, F., Wang, J., Wei, X., Xu, X., Yan, Z., Yang, F., Zhong, X., Zhou, F., Zhu, Y., Zhang, Y., Ayyampalayam, S., Barkman, T.J., phuong Nguyen, N., Matasci, N., Nelson, D.R., Sayyari, E., Wafula, E.K., Walls, R.L., Warnow, T., An, H., Arrigo, N., Baniaga, A.E., Galuska, S., Jorgensen, S.A., Kidder, T.I., Kong, H., Lu-Irving, P., Marx, H.E., Qi, X., Reardon, C.R., Sutherland, B.L., Tiley, G.P., Welles, S.R., Yu, R., Zhan, S., Gramzow, L., Theißen, G., Wong, G.K.S., 2019. One thousand plant transcriptomes and the phylogenomics of green plants. Nature 574, 679–685.

Li, H.T., Yi, T.S., Gao, L.M., Ma, P.F., Zhang, T., Yang, J.B., Gitzendanner, M.A., Fritsch, P.W., Cai, J., Luo, Y., Wang, H., van der Bank, M., Zhang, S.D., Wang, Q.F., Wang, J., Zhang,

Z.R., Fu, C.N., Yang, J., Hollingsworth, P.M., Chase, M.W., Soltis, D.E., Soltis, P.S., Li, D.Z., 2019. Origin of angiosperms and the puzzle of the Jurassic gap. Nature Plants 5, 461–470.

Ligas, J., Pineau, E., Bock, R., Huynen, M.A., Meyer, E.H., 2019. The assembly pathway of complex I in Arabidopsis thaliana. Plant Journal 97, 447–459.

Liu, S.L., Zhuang, Y., Zhang, P., Adams, K.L., 2009. Comparative analysis of structural diversity and sequence evolution in plant mitochondrial genes transferred to the nucleus. Molecular Biology and Evolution 26, 875–891.

Maclean, A.E., Hertle, A.P., Ligas, J., Bock, R., Balk, J., Meyer, E.H., 2018. Absence of Complex I Is Associated with Diminished Respiratory Chain Function in European Mistletoe. Current Biology 28, 1614-1619.e3.

Maldonado, M., Guo, F., Letts, J.A., 2021. Atomic structures of respiratory complex III2, complex IV, and supercomplex III2-IV from vascular plants. Elife 10, e62047.

Meyer, E.H., Welchen, E., Carrie, C., 2019. Assembly of the Complexes of the Oxidative Phosphorylation System in Land Plant Mitochondria. Annual Review of Plant Biology 70, 23–50.

Millar, A.H., Whelan, J., Soole, K.L., Day, D.A., 2011. Organization and Regulation of Mitochondrial Respiration in Plants. Annual Review of Plant Biology 62, 79–104.

Mower, J.P., Jain, K., Hepburn, N.J., 2012. Chapter Three - The Role of Horizontal Transfer in Shaping the Plant Mitochondrial Genome, in: Maréchal-Drouard, L. (Ed.), Advances in Botanical Research. Academic Press, pp. 41–69.

Nickrent, D.L., 2020. Parasitic angiosperms: How often and how many? Taxon 69, 5–27.

Nielsen, R., 2005. Molecular signatures of natural selection. Annual Review of Genetics 39, 197–218.

Palmer, J.D., Herbon, L.A., 1988. Journal of Molecular Evolution Plant Mitochondrial DNA Evolves Rapidly in Structure, but Slowly in Sequence. J Mol Evol 28, 87–97.

Piller, L.E., Besagni, C., Ksas, B., Rumeau, D., Bréhélin, C., Glauser, G., Kessler, F., Havaux, M., 2011. Chloroplast lipid droplet type II NAD(P)H quinone oxidoreductase is essential for prenylquinone metabolism and vitamin K 1 accumulation. Proceedings of the National Academy of Sciences of the United States of America 108, 14354–14359.

Rayapuram, N., Hagenmuller, J., Grienenberger, J.M., Giegé, P., Bonnard, G., 2007. AtCCMA interacts with AtCcmB to form a novel mitochondrial ABC transporter involved in cytochrome C maturation in Arabidopsis. Journal of Biological Chemistry 282, 21015–21023.

Rockenbach, K., Havird, J.C., Grey Monroe, J., Triant, D.A., Taylor, D.R., Sloan, D.B., 2016. Positive selection in rapidly evolving plastid-nuclear enzyme complexes. Genetics 204, 1507–1522.

Röhricht, H., Schwartzmann, J., Meyer, E.H., 2021. Complexome profiling reveals novel insights into the composition and assembly of the mitochondrial ATP synthase of Arabidopsis thaliana. Biochimica et Biophysica Acta - Bioenergetics 1862.

Roulet, M.E., Garcia, L.E., Gandini, C.L., Sato, H., Ponce, G., Sanchez-Puerta, M.V., 2020. Multichromosomal structure and foreign tracts in the Ombrophytum subterraneum (Balanophoraceae) mitochondrial genome. Plant Molecular Biology.

Sabar, M., De Paepe, R., De Kouchkovsky, Y., 2000. Complex I impairment, respiratory compensations, and photosynthetic decrease in nuclear and mitochondrial male sterile mutants of Nicotiana sylvestris. Plant Physiology 124, 1239–1249.

Sanchez-Puerta, M.V., Edera, A., Gandini, C.L., Williams, A.V., Howell, K.A., Nevill, P.G., Small, I., 2019. Genome-scale transfer of mitochondrial DNA from legume hosts to the holoparasite Lophophytum mirabile (Balanophoraceae). Molecular Phylogenetics and Evolution 132, 243–250.

Sanchez-Puerta, M.V., Garcia, L.E., Wohlfeiler, J., Ceriotti, L.F., 2017. Unparalleled replacement of native mitochondrial genes by foreign homologs in a holoparasitic plant. New Phytologist 214, 376–387.

Santos, H.J., Makiuchi, T., Nozaki, T., 2018. Reinventing an Organelle: The Reduced Mitochondrion in Parasitic Protists. Trends in Parasitology 34, 1038–1055.

Sato, H.A., 2014. Anatomía reproductiva de las especies de Lophophytum Schott & Endl.(Balanophoraceae) de la Argentina y revisión taxonómica del género en América. PhD thesis, Facultad de Ciencias Agrarias, Universidad Nacional del Nordeste, Corrientes, Argentina.

Schägger, H., Pfeiffer, K., 2000. Supercomplexes in the respiratory chains of yeast and mammalian mitochondria. EMBO Journal 19, 1777–1783.

Schelkunov, M.I., Nuraliev, M.S., Logacheva, M.D., 2019. Rhopalocnemis phalloides has one of the most reduced and mutated plastid genomes known. PeerJ 2019.

Schikowsky, C., Senkler, J., Braun, H.P., 2017. SDH6 and SDH7 contribute to anchoring succinate dehydrogenase to the inner mitochondrial membrane in arabidopsis thaliana. Plant Physiology 173, 1094–1108.

Senkler, J., Senkler, M., Eubel, H., Hildebrandt, T., Lengwenus, C., Schertl, P., Schwarzländer, M., Wagner, S., Wittig, I., Braun, H.P., 2017. The mitochondrial complexome of Arabidopsis thaliana. Plant Journal 89, 1079–1092.

Sloan, D.B., Triant, D.A., Wu, M., Taylor, D.R., 2014. Cytonuclear interactions and relaxed selection accelerate sequence evolution in organelle ribosomes. Molecular Biology and Evolution 31, 673–682.

Soucy, S.M., Huang, J., Gogarten, J.P., 2015. Horizontal gene transfer: Building the web of life. Nature Reviews Genetics 16, 472–482.

Stamatakis, A., 2014. RAxML version 8: A tool for phylogenetic analysis and post-analysis of large phylogenies. Bioinformatics 30, 1312–1313.

Su, H.J., Barkman, T.J., Hao, W., Jones, S.S., Naumann, J., Skippington, E., Wafula, E.K., Hu, J.M., Palmer, J.D., DePamphilis, C.W., 2019. Novel genetic code and record-setting AT-richness in the highly reduced plastid genome of the holoparasitic plant Balanophora. Proceedings of the National Academy of Sciences of the United States of America 116, 934–943.

Su, H.J., Hu, J.M., Anderson, F.E., Der, J.P., Nickrent, D.L., 2015. Phylogenetic relationships of Santalales with insights into the origins of holoparasitic Balanophoraceae. Taxon 64, 491–506.

Sun, F., Huo, X., Zhai, Y., Wang, A., Xu, J., Su, D., Bartlam, M., Rao, Z., 2005. Crystal structure of mitochondrial respiratory membrane protein Complex II. Cell 121, 1043–1057.

Sweetman, C., Waterman, C.D., Rainbird, B.M., Smith, P.M.C., Jenkins, C.D., Day, D.A., Soolea, K.L., 2019. Atndb2 is the main external NADH dehydrogenase in mitochondria and is important for tolerance to environmental stress. Plant Physiology 181, 774–788.

The Angiosperm Phylogeny Group, Chase, M.W., Christenhusz, M.J.M., Fay, M.F., Byng, J.W., Judd, W.S., Soltis, D.E., Mabberley, D.J., Sennikov, A.N., Soltis, P.S., Stevens, P.F., 2016. An update of the Angiosperm Phylogeny Group classification for the orders and families of flowering plants: APG IV. Botanical Journal of the Linnean Society 181, 1–20.

Tian, R.M., Cai, L., Zhang, W.P., Cao, H.L., Qian, P.Y., 2015. Rare events of intragenusand intraspecies horizontal transfer of the 16S rRNA gene. Genome Biology and Evolution 7, 2310–2320.

Touzet, P., Meyer, E.H., 2014. Cytoplasmic male sterility and mitochondrial metabolism in plants. Mitochondrion 19, 166–171.

Ukolova, I.V., Kondakova, M.A., Kondratov, I.G., Sidorov, A.V., Borovskii, G.B., Voinikov, V.K., 2020. New insights into the organisation of the oxidative phosphorylation system in the example of pea shoot mitochondria. Biochimica et Biophysica Acta - Bioenergetics 1861, 148264.

Weaver, R.J., Carrion, G., Nix, R., Maeda, G.P., Rabinowitz, S., Iverson, E.N.K., Thueson, K., Havird, J.C., 2020. High mitochondrial mutation rates in Silene are associated with nuclear-mediated changes in mitochondrial physiology. Biology Letters 16, 20200450.

Weng, M.L., Ruhlman, T.A., Jansen, R.K., 2016. Plastid–nuclear interaction and accelerated coevolution in plastid ribosomal genes in Geraniaceae. Genome Biology and Evolution 8, 1824–1838.

Williams, A.M., Friso, G., van Wijk, K.J., Sloan, D.B., 2019. Extreme variation in rates of evolution in the plastid Clp protease complex. Plant Journal 98, 243–259.

Williams, D., Gogarten, J.P., Papke, R.T., 2012. Quantifying homologous replacement of loci between haloarchaeal species. Genome Biology and Evolution 4, 1223–1244.

Yang, Z., 2007. PAML 4: Phylogenetic analysis by maximum likelihood. Molecular Biology and Evolution 24, 1586–1591.

Zervas, A., Petersen, G., Seberg, O., 2019. Mitochondrial genome evolution in parasitic plants. BMC Evolutionary Biology 19, 1–14.

Zhang, J., Ruhlman, T.A., Sabir, J., Blazier, J.C., Jansen, R.K., 2015. Coordinated rates of evolution between interacting plastid and nuclear genes in geraniaceae. Plant Cell 27, 563–573.

TABLES

Table 1. Nuclear genes involved in OXPHOS, ccm system, and alternative respiratory pathways in *Arabidopsis* and *Lophophytum mirabile*. Shown are the ORF lengths and estimated ratios of synonymous (dS) and non-synonymous (dN) substitution rates (ω = dN/dS) of the nuclear genes of *Lophophytum*.

FIGURE LEGENDS

Figure 1. Example of a native nuclear-encoded gene in *Lophophytum mirabile*. Maximum Likelihood (ML) phylogenetic analysis of the gene for the SDH1 subunit present in complex II of OXPHOS. ML bootstrap support values ≥50% from 1,000 bootstrap replicates are shown above each branch. The scale bar corresponds to substitutions per site. *Lophophytum* and Fabaceae sequences are in blue and orange, respectively.

Figure 2. Example of a foreign nuclear-encoded gene in *Lophophytum mirabile*. Maximum likelihood (ML) phylogenetic analysis of the gene for the SDH3 subunit present in the complex II of the OXPHOS. ML bootstrap support values ≥50% from 1,000 bootstrap replicates are shown above each branch. The scale bar corresponds to substitutions per site. *Lophophytum* and Fabaceae sequences are in blue and orange, respectively. Mt: mitochondrial-encoded genes; Nu: nuclear-encoded genes.

Figure 3. Schematic structure of the mosaic OXPHOS and ccm system in the inner mitochondrial membrane of *Lophophytum*, as well as that of the alternative respiratory pathways. Nuclear encoded genes are shown in light and dark indigo if native or foreign, respectively. Mitochondrial encoded genes are shown in light and dark purple if native or foreign/chimeric, respectively. The association of the plant-specific subunit COX1-X1 within complex IV is still unclear and is not shown.

SUPPLEMENTARY MATERIAL

Table S1. Accession numbers and references of the nuclear sequences included in the phylogenetic analyses.

Figure S1. Maximum likelihood phylogenetic analyses of the nuclear-encoded genes involved in OXPHOS, ccm system, and alternative respiratory pathways. Homologs of *Lophophytum mirabile* are all native, except for *sdh3*. ML bootstrap support values ≥50% from 1,000 bootstrap replicates are shown above each branch. Scale bars correspond to substitutions per site. *Lophophytum* and Fabaceae sequences are in blue and orange, respectively.

DATA

Data set 1. Nucleotide sequences of the *Lophophytum* ORFs identified in the assembled transcripts that code for subunits of the OXPHOS complexes, the maturation system of type c cytochromes, alternative oxidoreductases, and the cytochrome c.

List of abbreviations
A – adenosine
A – absorbance (1 cm)
aa – amino acid(s)
Ab – antibody(ies)
Ad – adenovirus
AdoMet (or SAM) – S-adenosylmethionine
AMV – avian myeloblastosis virus
Ap – ampicillin
βGal – β-galactosidase
bp – base pair(s)
BSA – bovine serum albumin
C – cytidine
cAMP – cyclic adenosine 3',5'-monophosphate
CAT – Cm acetyltransferase
cat – gene encoding CAT
ccc – covalently closed circular
cDNA – DNA complementary to RNA
CHO – Chinese hamster ovary
CIAP – calf intestinal alkaline phosphatase
Cm – chloramphenicol
cp – chloroplast
cpm – counts per minute
d – deoxyribo
Δ – deletion
dd – dideoxyribo
DMSO – dimethylsulfoxide
DNase – deoxyribonuclease
dNTP – deoxyribonucleoside triphosphate
ds – double strand(ed)
DTT – dithiothreitol
EF – elongation factor
ELISA – enzyme-linked immunosorbent assay
ENase (or R·) – restriction endonuclease
Er – erythromycin
EtdBr – ethidium bromide
G – guanosine
Gm – gentamicin
G418 – Geneticin
HIV – human immunodeficiency virus
HPLC – high-performance liquid chromatography

HPRT – hypoxanthine-guanine phosphoribosyl transferase
HSV – Herpes simplex virus
Hy – hygromycin
IF – initiation factor
IFN – Interferon
Ig – immunoglobulin(s)
IL – interleukin
IPTG – isopropyl β -D-thiogalactopyranoside
IS – insertion sequence(s)
kb – kilobase(s) or 1000 bp
kDa – kilodalton(s)
Km – kanamycin
lacZpo – lac promoter-operator
LB – Luria-Bertani (medium)
LTR – long terminal repeat(s)
m6A – N 6-methyladenosine
mAb – monoclonal Ab
MCS – multiple cloning site(s)
moi – multiplicity of infection
Mr – relative molecular mass (dimensionless)
mt – mitochondria(l)

MTase (or M ·) – DNA methyltransferase
Myr – million years
N – any nucleoside
NAD NADH – nicotinamide-adenine dinucleotide and its reduced form
Nm – neomycin
nt – nucleotide(s)
o, O – operator
oligo – oligodeoxyribonucleotide
ONPG – o-nitrophenyl β-D-galactopyranoside
ORF – open reading frame
ori – origin(s) of DNA replication
p – plasmid
p, P – promoter
PA – polyacrylamide
PAGE – PA-gel electrophoresis
PEG – poly(ethylene glycol)
pfu – plaque-forming unit(s)
Pi – inorganic phosphate
Pipes – 1,4-piperazinediethanesulfonic acid
PMSF – phenylmethylsulfonyl fluoride

Pollk – Klenow (large) fragment of E. coli DNA polymerase I
PPi – inorganic pyrophospate
PPO – 2,5-diphenyloxazole
R – (superscript) resistance/resistant
R – purine (or restriction)
RBS – ribosome-binding site(s)
rDNA – DNA coding for rRNA
re- – recombinant
RFLP – restriction-fragment length polymorphism
Rif – rifampicin
RNase – ribonuclease
rRNA – ribosomal RNA
s – (superscript) sensitivity/sensitive
S – sedimentation constant
SD – Shine-Dalgarno (sequence)
SDS – sodium dodecyl sulfate
Sm – streptomycin
ss – single strand(ed)
SSC – 0.15 M NaCl/0.015 M Na3·citrate pH 7.6
T – thymidine
t, T – terminator of transcription
Tc – tetracycline
Th – thiostrepton
TK – thymidine kinase
TMV – tobacco mosaic virus
Tn – transposon
tsp – transcription start point(s)
u – unit(s)
U – uridine
URF – unidentified open reading frame
UTR – unstranslated region(s)
UV – ultraviolet
wt – wild type
Xgal – 5-bromo-4-chloro-3-indolyl β-D-galactopyranoside
Y – pyrimidine
[ ] – denotes plasmid-carrier state
( ) – denotes prophage (lysogenic) state
:: – novel junction (fusion or insertion)
′ (prime) – denotes a truncated gene at the indicated side
Nucleotide symbol combinations:
Pairs: K = G/T; M = A/C; R = A/G; S = C/G; W = A/T; Y = C/T.
Triples: B = C/G/T; D = A/G/T; H = A/C/T; V = A/C/G; N=A/C/G/T.

HIGHLIGHTS

- *Lophophytum* has nearly complete and likely functional OXPHOS and ccm system
- All nuclear genes of the OXPHOS and ccm system are native, except for *sdh3*
- The highly chimeric mitochondrial complexes may be less efficient in *Lophophytum*
- Co-acquisition of *sdh3* and *sdh4* may be a case of cooperation between foreign genes

CREDIT AUTHOR STATEMENT

L. M. Gatica-Soria: Data Curation, Formal Analysis, Original Draft Preparation, Visualization. L. F. Ceriotti: Investigation, Writing, Reviewing and Editing. L. E. Garcia: Supervision, Writing, Reviewing and Editing. M.V. Sanchez-Puerta: Conceptualization, Supervision, Writing, Reviewing and Editing.

Declaration of interests

☐ The authors declare that they have no known competing financial interests or personal relationships that could have appeared to influence the work reported in this paper.

☒ The authors declare the following financial interests/personal relationships which may be considered as potential competing interests:

Maria Virginia Sanchez-Puerta reports financial support was provided by National Agency for Scientific and Technological Promotion. Maria Virginia Sanchez-Puerta reports financial support was provided by National University of Cuyo.